Boundary-Layer Similar Solutions for Equilibrium Dissociated Air and Application to the Calculation of Laminar Heat-Transfer Distribution on Blunt Bodies in High-Speed Flow

Nathaniel B. Cohen
Ivan E. Beckwith
NASA Langley Research Center
Langley Field, Virginia

ABSTRACT

Locally similar solutions to the laminar boundary-layer equations for a yawed infinite cylinder or a body of revolution at zero angle of attack are presented for equilibrium dissociated air. Exact solutions representing isothermal flat plate and stagnation flows are also presented and correlating formulas are derived for the appropriate heat-transfer coefficients. From the locally similar solutions, a correlation formula is deduced for application to a method of calculating heat-transfer distribution on blunt bodies with cooled walls.

NOMENCLATURE

C = mass concentration

c_f = skin-friction coefficient, $\dfrac{\tau_w}{\frac{1}{2}\rho_e u_e^2}$

c_p = frozen specific heat at constant pressure

F = diffusion function, (3)

f' = chordwise velocity profile, $\dfrac{u}{u_e}$

g = spanwise velocity profile, $\dfrac{v}{v_e}$

H = total enthalpy, $h + \dfrac{u^2}{2} + \dfrac{v^2}{2}$

h = static enthalpy

h_E = reference enthalpy, $250\bar{R}T_{\text{ref}}$

$\bar{h}$ = similarity heat-transfer coefficient, $\dfrac{\zeta'_w}{(\zeta_{aw} - \zeta_w)}$

j = exponent, 0 for yawed infinite cylinder, 1 for body of revolution

k = frozen conductivity

L = reference length

M = Mach number

M_∞ = free-stream or flight Mach number

N_{Le} = Lewis number

$N_{Nu,w}$ = Nusselt number, $\dfrac{q_w c_{p,w} x}{k_w (h_{aw} - h_w)}$

N_{Pr} = frozen Prandtl number, $\dfrac{\mu c_p}{k}$

N_{Re} = Reynolds number, $\dfrac{\rho_e u_e x}{\mu_e}$

$N_{Re,w}$ = Reynolds number, $\dfrac{\rho_w u_e x}{\mu_w}$

N_{St} = Stanton number, $\dfrac{q_w}{\rho_e u_e (h_{aw} - h_w)}$

P, Q, R, N = functions of t_s in correlation equation, (19)

$\bar{P}, \bar{Q}, \bar{R}, \bar{N}$ = corresponding functions from correlations of [1]

p = pressure

q = heat-transfer rate

$\bar{q}_w$ = surface heat-transfer coefficient, $\dfrac{q_w}{(h_{aw} - h_w)}$

$\bar{R}$ = gas constant for undissociated air

r = radius of body of revolution

$\bar{r}$ = enthalpy recovery factor, $\dfrac{(h_{aw} - h_e)}{(H_e - h_e)}$

T_{ref} = reference temperature, 273.16 K

t = dimensionless static enthalpy, $\frac{h}{H_e}$

$t_E = \frac{h_E}{H_e}$

t^* = reference enthalpy ratio, (12)

u, v, w = velocity components in the x, y, z directions, respectively

V_∞ = free-stream or flight velocity

x, y, z = physical boundary-layer coordinates (fig. 1)

β = velocity gradient parameter, (4)

Γ = function defined by (2)

γ = ratio of specific heats

ζ = total enthalpy ratio, $\frac{H}{H_e}$

η = similarity coordinate normal to surface, [1]

θ = angular position on circular cylinder from stagnation line

Λ = yaw or sweep angle

μ = viscosity

ξ = similarity coordinate in x-direction [1]

ρ = density

$\varphi = \frac{\rho\mu}{\rho_w\mu_w}$

Subscripts

A, M = atoms, molecules

aw = insulated wall

e = local value external to the boundary layer

s = stagnation point or line, where $u_e = 0$

w = local wall conditions

Superscripts

$'$ = differentiation with respect to η

$*$ = evaluated at reference enthalpy ratio, t^*

1. INTRODUCTION

The purpose of the present paper is to present correlation equations obtained from a large body of similar solutions of the laminar boundary-layer equations for air in dissociation equilibrium. These correlations are applied to the integral and simple local similarity methods of computing heat-transfer distribution presented in [1], wherein similar solutions for a perfect gas with viscosity proportional to temperature and unit Prandtl number were instead utilized. Flat-plate and stagnation-flow heat-transfer coefficients are also presented for equilibrium dissociated air. The transport properties used are those of Hansen [2] as correlated in [3].

Extension of the results of the present locally similar solutions and the methods for computing heat-transfer distribution to the case of blunt three-dimensional bodies [4, 5, and 6] is briefly discussed.

2. EQUATIONS FOR HEAT-TRANSFER DISTRIBUTION

The heat-transfer distribution on blunted yawed infinite cylinders or bodies of revolution predicted by the integral method of [1] may be expressed for equilibrium dissociated air as

$$\frac{q_w}{q_{w,s}} = \left[\frac{\frac{\rho_w\mu_w}{\beta t_e}\frac{du_e}{dx}}{\left(\frac{\rho_w\mu_w}{\beta t_e}\frac{du_e}{dx}\right)_s}\right]^{1/2} \Gamma \qquad (1)$$

where

$$\Gamma = \frac{\frac{1+F_w}{N_{Pr,w}}}{\left(\frac{1+F_w}{N_{Pr,w}}\right)_s}\frac{\zeta'_w}{\zeta'_{w,s}} \qquad (2)$$

$$F = (N_{Le} - 1)(h_A - h_M)\left(\frac{\partial C_A}{\partial h}\right)_p \qquad (3)$$

and

$$\beta = \frac{2t_s\frac{du_e}{dx}}{\rho_w\mu_w u_e^2 t_e\left(\frac{r}{L}\right)^{2j}\Gamma^2}\int_0^x \rho_w\mu_w u_e\left(\frac{r}{L}\right)^{2j}\Gamma^2\,dx \qquad (4)$$

The coordinate systems are shown in Figure 1. For the yawed infinite cylinder, t_s (the ratio of inviscid

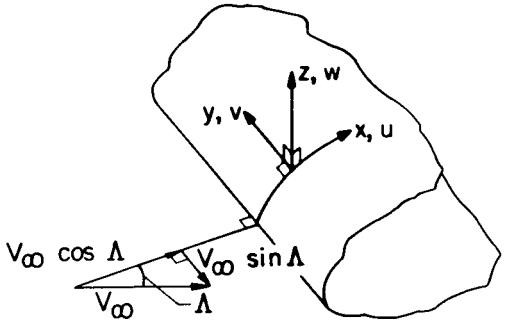

(a) Coordinates for the yawed infinite cylinder

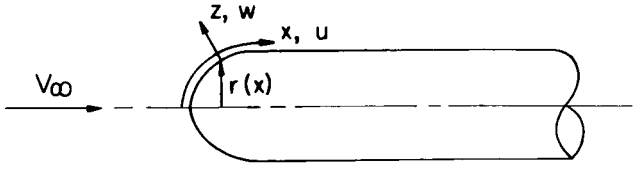

(b) Coordinates for the body of revolution

FIG. 1 - BOUNDARY-LAYER COORDINATE SYSTEMS.

stagnation line enthalpy to total enthalpy) is a constant given by

$$t_s = \frac{h_s}{H_e} = 1 - \frac{v_e^2}{2H_e} = 1 - \frac{V_\infty^2 \sin^2 \Lambda}{2H_e} \tag{5}$$

For the body of revolution, $j = 1$, $v_e = 0$, and hence $t_s = 1$.

Equations (1) to (4) result from the application of locally similar profiles at each station with the requirement that the integrated energy equation is satisfied. Because $\frac{\zeta'_w}{\zeta'_{w,s}}$ (the ratio of local to stagnation values of the surface enthalpy gradient which must be obtained from locally similar solutions of the boundary-layer equations) is a function of β, (2) and (4) must be solved by iteration at each station.

If Γ is set equal to unity in (4) only, (1) to (4) reduce essentially to the method of local similarity, [7]. If Γ is unity in both (1) and (4), these equations are essentially the same as those of [8].

Although (1) to (4) were derived in [1] for equilibrium dissociated air, similar solutions of the boundary-layer equations for a perfect gas with a linear viscosity-temperature relation and unit Prandtl number were utilized therein for the determination of the dependence of $\frac{\zeta'_w}{\zeta'_{w,s}}$ upon β as well as on the other parameters. In the following sections similar solutions for air in dissociation equilibrium are presented for application to (1) to (4).

3. SIMILAR SOLUTIONS

The Differential Equations for Equilibrium Dissociated Air. The governing differential equations for locally similar profiles are [1]

$$(\varphi f'')' + f f'' =$$

$$\beta \left[(f')^2 - \frac{\zeta}{t_s} + \frac{1 - t_s}{t_s} g^2 - \frac{t_e}{t_s} \left(\frac{\rho_e}{\rho} - \frac{t}{t_e} \right) \right] \tag{6}$$

$$(\varphi g')' + f g' = 0 \tag{7}$$

$$\left[\frac{\varphi}{N_{Pr}} (1 + F) \zeta' \right]' + f \zeta' =$$

$$\left\{ \frac{\varphi}{N_{Pr}} (1 - N_{Pr} + F) [(t_s - t_e)(f')^{2'} + (1 - t_s)(g^2)'] \right\}' \tag{8}$$

with the boundary conditions

$$f(0) = f'(0) = g(0) = 0 \tag{9a}$$

$$\left.\begin{aligned} &\zeta(0) = \zeta_w \text{ (Heat transfer)} \\ \text{or} \quad &\zeta'(0) = 0 \text{ (Insulated wall)} \end{aligned}\right\} \tag{9b}$$

and

$$f'(\infty) = g(\infty) = \zeta(\infty) = 1 \tag{9c}$$

Equations (6) to (8), subject to the boundary conditions, (9), were programed on the IBM type 704 electronic data processing machine along with the necessary auxiliary equations and the gas properties φ, $\frac{\rho_e}{\rho}$, N_{Pr}, and F from (3) and (6) and Table I of [3]. Parameters were β, t_s, t_e, t_E, and ζ_w. All cases computed followed the limitation set by the transport property functions of [3] on the static enthalpy; that is, that $0.0152 \leqq \frac{h}{h_E} \leqq 2$ throughout the boundary layer. The upper limit corresponds to the stagnation enthalpy for flight at about 29,000 ft/sec. In addition, for those cases with $t_s < 1$, the maximum velocity was set at 35,600 ft/sec. Lastly, the wall temperature was always between 300 K and about 1,750 K for heat-transfer cases.

Exact Similar Flows. For flat-plate flows, axisymmetric stagnation point flows, and stagnation line flows for the yawed infinite cylinder, solutions of (6) to (8) yield the appropriate exact boundary-layer profiles because, in these cases, no variation with ξ is present. Solutions for these cases will be discussed first.

Flat-plate Flow. With $\beta = 0$, (6) to (8) represent the flow over an isothermal flat plate. For this case, since $g(\eta) = f'(\eta)$, all dependence upon t_s drops from the equations, which were solved (with $F = 0$) for a wide variety of cases up to a stagnation enthalpy, $\frac{H_e}{h_E}$, equal to 2 (up to a flight speed of 29,000 ft/sec). It was found that the skin-friction function, $c_f \sqrt{N_{Re}}$, correlated with the quantity $\frac{\rho_e \mu_e}{\rho_w \mu_w}$ independent of the level of the total enthalpy. Some of the results are shown in Figure 2, where values of the parameter t_e indicate the velocity or Mach number effect. It was found that the reference enthalpy method of Eckert, [9], used with the gas property correlations of [3], predicted skin-friction coefficients lower than the results of the exact solutions by at most 5 percent, and is thus a good approximation for flat-plate skin-friction coefficients for equilibrium dissociated air. The equations for this approximation are

$$c_f \sqrt{N_{Re}} = 0.664 \sqrt{\frac{\rho^* \mu^*}{\rho_e \mu_e}} \tag{10}$$

$$\frac{\rho^* \mu^*}{\rho_e \mu_e} = \frac{1.0213 \left(\frac{t_e}{t_E} \right)^{0.3329} - 0.0213}{1.0213 \left(\frac{t^*}{t_E} \right)^{0.3329} - 0.0213} \tag{11}$$

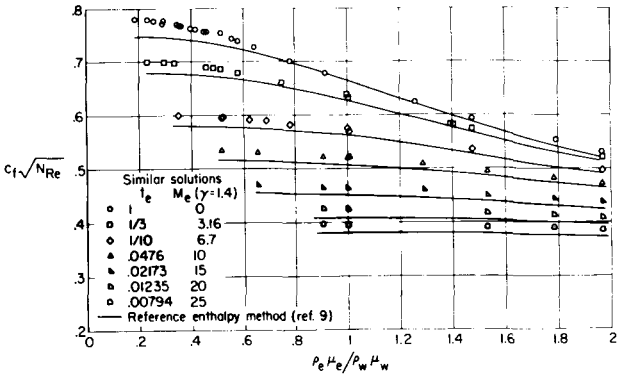

FIG. 2 - LAMINAR FLAT-PLATE SKIN-FRICTION COEFFICIENT AS A FUNCTION OF $\rho_e \mu_e/\rho_w \mu_w$ FOR EQUILIBRIUM DISSOCIATED AIR. $N_{Le} = 1$.

$$\frac{t^*}{t_E} = \frac{t_e}{t_E}\left[0.5\left(1 + \frac{\zeta_w}{t_e}\right) - 0.22\bar{r}\left(1 - \frac{1}{t_e}\right)\right] \quad (12)$$

where $\bar{r}$ is the enthalpy recovery factor, assumed here as equal to $\sqrt{0.7}$ for simplicity. It was also found from the numerical solutions that a Reynolds analogy in the form

$$\frac{N_{St}}{c_f} = \frac{1}{2}(N^*_{Pr})^{-2/3} \quad (13)$$

was valid within ±4 percent for the entire range of the parameters t_e, t_E, and ζ_w. In computing the Stanton number, an enthalpy recovery factor of $\sqrt{N^*_{Pr}}$ was used because it was a slightly better approximation than was the nominal value $\sqrt{0.7}$ to the exact values, which varied from 0.82 to 0.86 for real air in those insulated wall cases computed during the present program.

The effect of variable Lewis number was investigated in a few cases by using the variable F table programed from [3], Table I. The effect on skin-friction coefficient was insignificant while the effect on heat transfer was to increase the Stanton number by less than 5 percent even at the highest velocities considered.

Axisymmetric Stagnation Flow. This problem requires $\beta = \frac{1}{2}$ and $t_s = t_e = 1$ in (6) and (8) (equation (7) need not be considered). With $F = 0$ (unit Lewis number), twenty-two heat-transfer cases were computed and the results for the Nusselt number parameter plotted in Figure 3. Shown also is the correlation function

$$\left[\frac{N_{Nu,w}}{(N_{Pr,w})^{0.4}(N_{Re,w})^{0.5}}\right]_s = 0.767\left(\frac{\rho_e \mu_e}{\rho_w \mu_w}\right)^{0.43}_s \quad (14)$$

which generally agrees with the numerical data within ±5 percent. It is noteworthy that the coefficient and exponent on the right-hand side of (14) are very little dependent upon the gas properties used in solutions of the differential equations obtained to date. For example, for the case of constant fluid properties (incompressible fluid), there are obtained the values 0.763 and 0.5, respectively [10], and for equilibrium dissociated air with $N_{Le} = 1$, constant N_{Pr}, and using the Sutherland viscosity relation, Fay and Riddell obtained 0.768 and 0.4, respectively [11]. Thus, this stagnation-point heat-transfer parameter is not greatly affected by real-air properties.

From the definitions of the Nusselt and Reynolds numbers, the aerodynamic heat-transfer rate, using (14) is

$$q_{w,s} = 0.767\,(N_{Pr,w})^{-0.6}_s (H_e - h_w)_s (\rho_e \mu_e)^{0.43}_s (\rho_w \mu_w)^{0.07}_s \sqrt{\left(\frac{du_e}{dx}\right)_s} \quad (15)$$

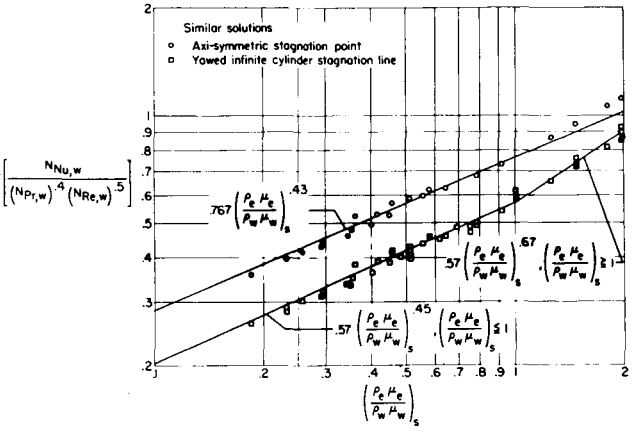

FIG. 3 - STAGNATION-FLOW HEAT-TRANSFER PARAMETER AS A FUNCTION OF $(\rho_e \mu_e/\rho_w \mu_w)_s$ FOR EQUILIBRIUM DISSOCIATED AIR. $N_{Le} = 1$.

since $h_{aw} = H_e$ for this case. Although the aforementioned coefficient and exponent are little influenced by gas properties, (15) indicates that the heat-transfer rate does depend upon the transport properties, especially upon the viscosity outside the boundary layer, $\mu_{e,s}$. Thus, as better estimates of the transport properties of equilibrium dissociated air become available, it should be possible to use (15) without further change provided the best estimate of the fluid properties is utilized.

For variable Lewis number the present calculations for a few high stagnation enthalpy cases indicate an increase in heat-transfer function of at most 5 percent. The results of [11] for $N_{Le} = 1.4$, on the other hand, indicate an increase of as much as 15 percent for fully dissociated air. Thus, if the Lewis number variation of [2] is reasonably correct, a non-unit Lewis number correction is unnecessary.

Stagnation Flow for a Yawed Infinite Cylinder. With $\beta = 1$ and $t_s = t_e \leqq 1$, (6) to (8) represent the

stagnation line boundary layer on a yawed infinite cylinder. With $F = 0$, 49 heat-transfer cases were computed with values of the yaw parameter, t_s, of 1, 1/3, 1/10, and 1/30. The results are shown on Figure 3 along with the correlating functions

$$\left[\frac{N_{Nu,w}}{(N_{Pr,w})^{0.4}\,(N_{Re,w})^{0.5}}\right]_s = \begin{cases} 0.57\left(\dfrac{\rho_e\mu_e}{\rho_w\mu_w}\right)_s^{0.45}, & \left(\dfrac{\rho_e\mu_e}{\rho_w\mu_w}\right)_s < 1 \\ 0.57\left(\dfrac{\rho_e\mu_e}{\rho_w\mu_w}\right)_s^{0.67}, & \left(\dfrac{\rho_e\mu_e}{\rho_w\mu_w}\right)_s > 1 \end{cases} \quad (16)$$

which fit the numerical data within about ±7 percent independent of the enthalpy level. In computing the Nusselt number parameter from the similar solutions for $t_s < 1$, an enthalpy recovery factor of 0.85 was used as an approximation to the exact values which varied from 0.84 to 0.88 for those insulated wall stagnation line cases computed in the present program. The value of 0.85 is also an excellent approximation for the stagnation line recovery factor for perfect air with the Sutherland viscosity relation and $N_{Pr} = 0.7$ [12].

Equation (16) may be compared with the result for perfect air (Sutherland viscosity) from [12],

$$\left[\frac{N_{Nu,w}}{(N_{Pr,w})^{0.4}\,(N_{Re,w})^{0.5}}\right]_s = 0.577\left(\frac{\rho_e\mu_e}{\rho_w\mu_w}\right)_s^{0.44} \quad (17)$$

and little effect of the gas properties is seen for $\left(\dfrac{\rho_e\mu_e}{\rho_w\mu_w}\right)_s < 1$. For $\left(\dfrac{\rho_e\mu_e}{\rho_w\mu_w}\right)_s > 1$, the present results and those of [12] do not compare as favorably.

The effect of variable Lewis number on the present results was found to be essentially the same as for the axisymmetric case, and thus is negligible.

Locally Similar Solutions for the Heat-Transfer Parameter. From (1) to (4), it is evident that the β distribution and heat-transfer distribution of the integral and local similarity methods of [1] depend upon the inviscid flow, the wall conditions, and the ratio $\dfrac{\zeta'_w}{\zeta'_{w,s}}$ as determined by locally similar solutions. To determine the dependence of ζ'_w upon the parameters β, t_e, t_s, ζ_w, and t_E, a large number of similar solutions (of (6) to (8)) were obtained using the gas properties already described with $F = 0$ ($N_{Le} = 1$). The parameters were varied independently over practical ranges, consistent with the limitations on the gas property functions already described. In addition, the limitation $0.2 \leqq \dfrac{t_e}{t_s} \leqq 1.0$, which should cover most practical cases, was set. Values of β from zero to about 3.5 were used. Above this limit, solutions of (6) to (8) generally were not obtained because of numerical difficulties. Lastly, values of t_s = 1, 1/3, 1/10, and 1/30 were investigated.

The effect of each parameter was determined by separating the function $\dfrac{\zeta'_w}{\zeta'_{w,s}}$ into various factors. Thus, at constant t_s and t_E (specified by flow conditions), ζ'_w may be written in functional form as $\zeta'_w(\beta, t_e, \zeta_w)$, and the ratio $\dfrac{\zeta'_w}{\zeta'_{w,s}}$ is

$$\frac{\zeta'_w}{\zeta'_{w,s}} = \frac{\zeta'_w(\beta, t_e, \zeta_w)}{\zeta'_w(\beta_s, t_s, \zeta_{w,s})} = \left[\frac{\zeta'_w(\beta, t_e, \zeta_w)}{\zeta'_w(\beta=1, t_e, \zeta_w)}\right]\left[\frac{\zeta'_w(\beta=1, t_e, \zeta_w)}{\zeta'_w(\beta=1, t_s, \zeta_w)}\right]\times \left[\frac{\zeta'_w(\beta=1, t_s, \zeta_w)}{\zeta'_w(\beta=1, t_s, \zeta_{w,s})}\right]\left[\frac{\zeta'_w(\beta=1, t_s, \zeta_{w,s})}{\zeta'_w(\beta_s, t_s, \zeta_{w,s})}\right] \quad (18)$$

Detailed analysis of the numerical solutions indicated that these factors could each be approximated by correlation formulas, and the following approximate formula for $\dfrac{\zeta'_w}{\zeta'_{w,s}}$ was determined,

$$\frac{\zeta'_w}{\zeta'_{w,s}} = \left\{\frac{1 + P\beta^N}{Q + R\beta^N}\left[1 + 0.050(1 - t_s)\left(1 - \frac{t_e}{t_s}\right)\times \left(\frac{\beta - 1}{0.2\beta + 1}\right)\right]\right\}\left\{\left[1.1 - 0.1625\frac{t_e}{t_s} + 0.0625\left(\frac{t_e}{t_s}\right)^2\right]\left(\frac{0.85 + 0.15t_e - \zeta_w}{0.85 + 0.15t_s - \zeta_{w,s}}\right)\right\}\times \left\{\left(\frac{N_{Pr,w}}{N_{Pr,w,s}}\right)^{0.4}\frac{[\varphi(t_s, \zeta_w)]^{0.45}}{[\varphi(t_s, \zeta_{w,s})]^{0.45}}\right\}[(1.033)^j] \quad (19)$$

valid for $\beta > 0$ and $\zeta_w/t_s \lesssim 1$ within about 15 percent. Values of P, Q, R, and N depended upon t_s as given in Table 1.

TABLE 1. DEPENDENCE OF P, Q, R, AND N UPON t_s FOR $\dfrac{\zeta_w}{t_s} \lesssim 1$

t_s	P	Q	R	N
1	0.527	1.116	0.411	0.686
1/3	.759	1.193	.566	.677
1/10	1.195	1.344	.851	.629
1/30	1.850	1.558	1.292	.612

The braces in (19) indicate the contribution of the corresponding factors in (18), and examples of

two of the individual correlation factors are shown in Figures 4 and 5. Equation (19) may be applied to the calculation of heat-transfer distribution on blunt yawed infinite cylinders ($j = 0$) or blunt bodies of revolution ($j = 1$).

The effect of nonunit Lewis number upon the function $\frac{\zeta'_{\dot{w}}}{\zeta'_{\dot{w},s}}$ was investigated for a few cases and found, as expected, negligible.

Equation (19) may be compared to the corresponding equation from [1] (based on $N_{Pr} = 1$ boundary-layer similar solutions). For two-dimensional flow with an isothermal wall, for example, (19) may be written as

$$\frac{\bar{h}}{\bar{h}_s} = \frac{\dfrac{\zeta'_{\dot{w}}}{(0.85 + 0.15\,t_e - \zeta_w)}}{\dfrac{\zeta'_{\dot{w},s}}{(0.85 + 0.15\,t_s - \zeta_w)}}$$

$$= \frac{1 + P\beta^N}{Q + R\beta^N}\left[1 + 0.050(1 - t_s)\left(1 - \frac{t_e}{t_s}\right) \times \left(\frac{\beta - 1}{0.2\beta + 1}\right)\right]\left[1.1 - 0.1625\,\frac{t_e}{t_s} + 0.0625\left(\frac{t_e}{t_s}\right)^2\right], \quad \frac{\zeta_w}{t_s} \lesssim 1 \qquad (20)$$

The corresponding expression from [1] is

$$\frac{\bar{h}}{\bar{h}_s} = \frac{1 + \bar{P}\beta^{\bar{N}}}{\bar{Q} + \bar{R}\beta^{\bar{N}}} \qquad (21)$$

where $\bar{P}$, $\bar{Q}$, $\bar{R}$, and $\bar{N}$ are given in the reference as functions of t_s and ζ_w. The only difference in the form of (20) and (21) is caused by dissipation (excluded in [1] through the $N_{Pr} = 1$ assumption), that is, the terms $\left(1 - \frac{t_e}{t_s}\right)$ and $\frac{t_e}{t_s}$ in (20). These effects are

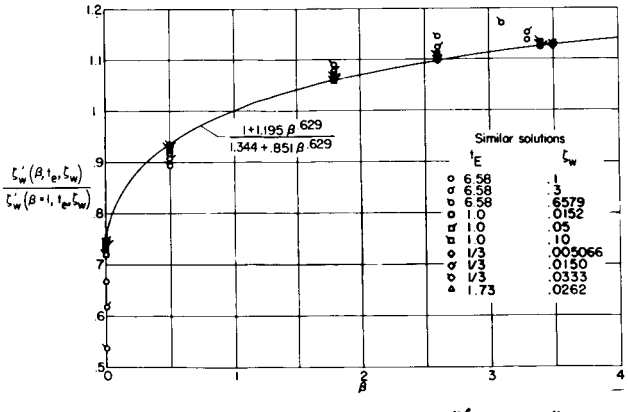

FIG. 4 - DEPENDENCE OF THE FACTOR $\zeta'_w(\beta, t_e, \zeta_w)/\zeta'_w(\beta = 1, t_e, \zeta_w)$ UPON β. $t_s = t_e = \frac{1}{10}$.

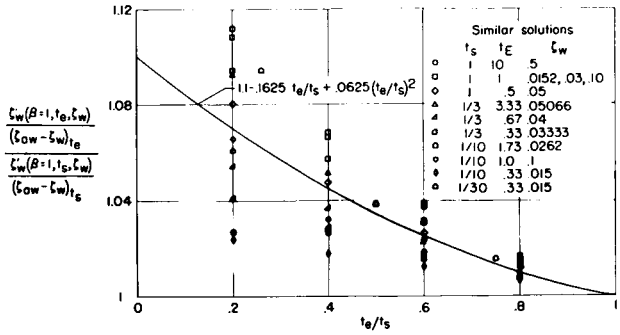

FIG. 5 - DEPENDENCE OF THE FACTOR $\dfrac{\zeta'_w(\beta = 1, t_e, \zeta_w)}{(\zeta_{aw} - \zeta_w)_{t_e}} \Big/ \dfrac{\zeta'_w(\beta = 1, t_s, \zeta_w)}{(\zeta_{aw} - \zeta_w)_{t_s}}$ UPON t_e/t_s. $\bar{r} = 0.85$.

primarily functions of the deviation of the real air Prandtl number from unity and are not necessarily a result of dissociation. As a result of the dissipation terms, the "real" air heat-transfer distribution (20) may exceed that for the $N_{Pr} = 1$ gas by up to about 7 percent for $\beta > 0$ with a highly cooled wall ($\zeta_w \approx 0$) and zero yaw, and up to about 18 percent for the corresponding case with large yaw. Differences in P and $\bar{P}$, Q and $\bar{Q}$, etc., contribute an additional few percent for $\beta > 1$ but tend to compensate for the dissipation effects when $\beta < 1$.

4. DISCUSSION

Comparison of Theory With Experiment for a Perfect Gas. In [1] it was shown for two shapes for which perfect gas test data were available that the perfect gas theory with $N_{Pr} = 1$ correlations predicted the measured heat-transfer distributions within the scatter of the data. The cases were an unyawed cylinder at freestream Mach numbers of 3.9 to 5.5 and a flat-faced cylinder (alined parallel to the flow) with a corner radius of 0.09 times the body radius at a Mach number of 6.2. Of particular interest was the fact that the integral method (1) to (4) and that of simple local similarity (the latter uses $\Gamma = 1$ in (4)) gave almost identical results for blunt bodies. Furthermore, in the region of large pressure gradient (the corner on the flat-faced model), both methods accurately predicted the experimental results contrary to the results reported in [7] for a similar body with a larger corner radius. It was concluded that for most practical cases, the method of local similarity (with $\Gamma = 1$ in (4)) is sufficiently accurate for the design of blunt reentry vehicles with large favorable pressure gradients.

No data with finite yaw angle were included in [1] but some low-temperature wind-tunnel data for $\Lambda = 70^\circ$ are now available. The experimental results are shown in Figure 6. The circles

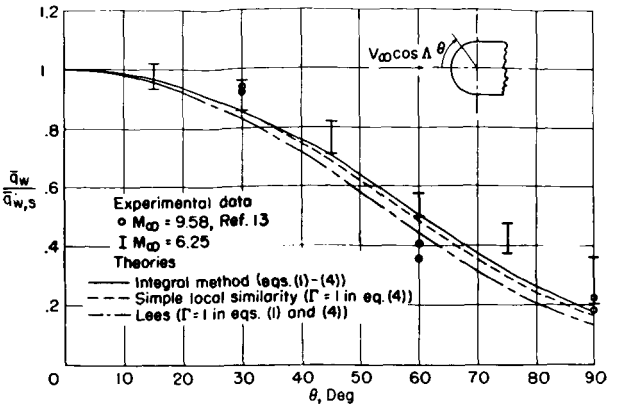

FIG. 6 - COMPARISON OF THEORETICAL AND EXPERIMENTAL HEAT-TRANSFER-COEFFICIENT DISTRIBUTIONS ON YAWED INFINITE CYLINDER. $\Lambda = 70°$.

represent some of the data from the sharp prow delta wing with cylindrical leading edge reported in [13] (Mach number 9.58), and the "I beams" represent the scatter limits in some unpublished data at a Mach number of 6.25 obtained by R. A. Jones at the Langley Research Center. Though the test Mach numbers differ, the theoretical results by the methods of [1] ((1) to (4) and (21)) are about the same for both test conditions and are shown on the figure as single curves for comparison with experiment. Unit Prandtl number, perfect gas correlations were again used because stagnation line temperatures for the tests were considerably below the 300 K lower limit of the present correlations. Over most of the cylinder the predictions are generally lower than the experimental results, a result partly attributed to the neglect of dissipation in the correlations of [1] discussed previously. These effects would be expected to occur even in a perfect gas with nonunit Prandtl number, and to judge by the present dissociated air solutions, might tend to increase the predicted heat-transfer distributions by about 10 to 15 percent in the downstream regions ($\theta \gtrsim 50°$). With this correction included, the present integral and local similarity methods would predict heat-transfer distributions just within the data scatter.

The results obtained using the method of Lees ($\Gamma = 1$ in (1) and (4)) are independent of Prandtl number and thus would be unaffected by the inclusion of dissipation. This prediction is lower than the mean of the data by as much as 50 percent at $\theta = 90°$ and the method is not recommended for large yaw cases.

A Numerical Example Using the Real Air Correlations. A numerical example was computed in [1] for a swept circular cylinder at a velocity of 15,500 ft/sec at 174,000 feet of altitude using the perfect gas ($N_{Pr} = 1$) correlations, but with the inviscid flow computed both for a perfect gas and for equilibrium air. It was found that for zero yaw ($t_s = 1$), the effect of the real air inviscid flow was to increase the heat-transfer distribution by at most 11 percent at a station 125° around from the stagnation line. For $t_s = 0.1$ ($\Lambda = 74°$), the effect of the real air inviscid flow was negligible. The same cases have been computed using the real air inviscid flow and the real air boundary-layer correlations of the present report (1) to (4) and (19) by the method of local similarity ($\Gamma = 1$ in (4)). The results are illustrated in Figure 7, where the ratio of real to perfect gas distribution is shown for both yaw angles.

With zero yaw, use of the real air correlations of the present report increases the heat-transfer distribution aft of about 60° a moderate amount, up to an 18-percent increase at 125°, relative to the distribution with a perfect gas inviscid flow and $N_{Pr} = 1$ correlations. Roughly half of this increase is attributed to the real air boundary-layer correlations themselves; the other half is caused by the use of the real air inviscid flow. At large yaw, where the use of the real air inviscid flow is of little consequence, the real air boundary-layer correlations cause an increase of up to 18 percent in the heat-transfer distribution, illustrating again the effect of dissipation rather than dissociation effects. In these cases, however, the largest dissipation effects occur in regions of relatively low heating rate.

Application to Three-Dimensional Flows. If the boundary-layer equations for a three-dimensional body are written in terms of an inviscid streamline coordinate system and if the cross flow is assumed small, the continuity, energy, and streamwise momentum equations are independent of the cross-flow velocity component and take the same form as the corresponding equations for axisymmetric flow [4]. Consequently, the heat transfer is independent of the cross

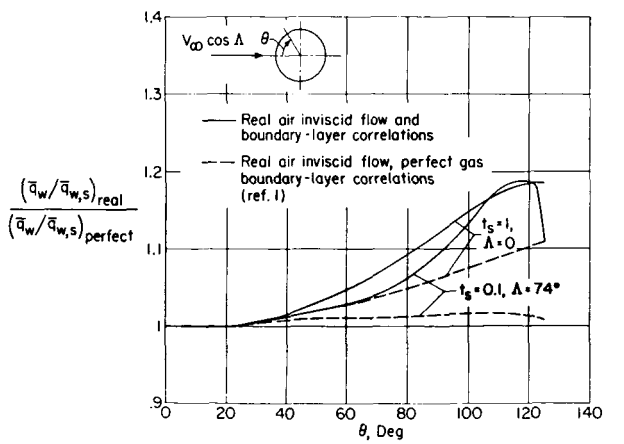

FIG. 7 - EFFECT OF REAL-AIR PROPERTIES UPON HEAT-TRANSFER-COEFFICIENT DISTRIBUTION FOR A YAWED INFINITE CYLINDER. V_∞ = 15,500 FT/SEC, 174,000 FEET ALTITUDE. $\zeta_w \ll 1$.

flow and may be computed by any method applicable to the axisymmetric case.

This approach was used in [5] where the method of Lees [8] was extended to the forward portion of a three-dimensional body with highly cooled walls. In the present method all equations for computing heat transfer remain the same except (4) where the factor $\left(\frac{r}{L}\right)^{2j}$ is replaced by the square of the normal spacing between adjacent streamlines and where x is the distance along a streamline.

The restrictions imposed in [5] are not always required for the valid application of the axisymmetric equations as shown in [6] where solutions to a reduced form of the cross-flow momentum equation were obtained. These solutions were utilized in [6] to define quantitatively the range of conditions where the small-cross-flow assumption is applicable. Comparisons with exact solutions for a yawed cylinder indicated that the small-cross-flow theory predicts heating distributions with good accuracy even when the cross flow is large.

5. CONCLUSIONS

Exact solutions to the laminar boundary-layer equations for flat plates and stagnation flows have been computed for air in dissociation equilibrium. For an isothermal flat plate, the skin-friction coefficient was shown well represented by the reference enthalpy method; a form of the Reynolds analogy was shown valid for the Stanton number. Solutions for the stagnation flow Nusselt number functions were found to be well represented by simple correlation formulas which are essentially independent of gas properties. The solutions, which were based on the transport properties of air as approximated in NASA Report R-50, indicated a negligible effect of nonunit Lewis number.

From locally similar solutions of the equations for arbitrary values of the pressure gradient, dissipation, yaw, enthalpy level, and wall enthalpy parameters, a correlation formula with an accuracy of about 15 percent was deduced for the heat-transfer distribution function appropriate to blunt yawed cylinders and bodies of revolution with cooled walls. The use of these results in the integral and simple local similarity methods of NASA TN D-625 for computing laminar heat-transfer distribution was shown. These methods, which were shown to predict experimental heat-transfer distributions very well for unyawed bodies in NASA TN D-625, were herein compared with experimental results for a perfect gas case with large yaw, and the theoretical results found to be somewhat lower than the experimental data, a result attributed partly to the neglect of dissipation in the perfect gas, unit Prandtl number boundary-layer solutions utilized in the computations. As in the unyawed case, use of the integral method gave no significant improvement over the local similarity method for large yaw.

The results for the body of revolution have application to the more general problem of heat-transfer distribution along the inviscid streamlines at the surface of a three-dimensional body provided that the cross flow is small. The possibility of relaxing the small-cross-flow restriction is briefly discussed.

REFERENCES

1. "Application of Similar Solutions to Calculation of Laminar Heat Transfer on Bodies With Yaw and Large Pressure Gradient in High Speed Flow," I. E. Beckwith and N. B. Cohen, NASA TN D-625, 1960.

2. "Approximations for the Thermodynamic and Transport Properties of High Temperature Air," C. F. Hansen, NASA Rep. R-50, 1959.

3. "Correlation Formulas and Tables of Density and Some Transport Properties of Equilibrium Dissociating Air for Use in Solutions of the Boundary Layer Equations," N. B. Cohen, NASA TN D-194, 1960.

4. "Boundary Layers in Three Dimensions," J. C. Cooke and M. G. Hall, R.A.E. Rep. AERO. 2635, 1960.

5. "Laminar Heat Transfer on Three-Dimensional Blunt Nosed Bodies in Hypersonic Flow," R. Vaglio-Laurin, *American Rocket Society Journal*, Vol. 29, no. 2, 1959, pp. 123–129.

6. "Similarity Solutions for Small Cross Flows in Laminar Compressible Boundary Layers," I. E. Beckwith, NASA Prospective TN, 1961.

7. "Laminar Heat Transfer Around Blunt Bodies in Dissociated Air," N. H. Kemp, P. H. Rose, and R. W. Detra, *Journal of the Aero/Space Sciences*, Vol. 26, no. 7, 1959, pp. 421–430.

8. "Laminar Heat Transfer Over Blunt-Nosed Bodies at Hypersonic Speeds," *L. Lees, Jet Propulsion*, Vol. 26, no. 4, 1956, pp. 259–269, 274.

9. "Survey on Heat Transfer at High Speeds," E. R. G. Eckert, Wright Aeronautical Development Center, Tech. Rep. 54–70, 1954.

10. "Heat Transfer Near the Forward Stagnation Point of a Body of Revolution," M. J. Sibulkin, *Journal of the Aeronautical Sciences*, Vol. 19, no. 8, 1952, pp. 570–571.

11. "Theory of Stagnation Point Heat Transfer in Dissociated Air," J. A. Fay and F. R. Riddell,

Journal of the Aeronautical Sciences, Vol. 25, no. 2, 1958, pp. 73–85.

12. "Similar Solutions for the Compressible Boundary Layer on a Yawed Cylinder With Transpiration Cooling," I. E. Beckwith, NASA Rep. R-42, 1959.

13. "Recent Hypersonic Studies of Wings and Bodies," M. H. Bertram and A. Henderson, Paper Presented at the American Rocket Society Semi-Annual Meeting, Ambassador Hotel, Los Angeles, California, May 9–12, 1960.

AUTHORS REPRINT*

*Presented at the 1961 International Heat Transfer Conference held August 28–September 1, 1961, University of Colorado, Boulder, Colorado, U.S.A. Papers presented for discussion at this meeting have been published in *International Developments in Heat Transfer* by The American Society of Mechanical Engineers, 29 West 39th Street, New York 18, N.Y.